SUPPLEMENTARY INFORMATION

Ultrafast Excited-State Dynamics of Rhenium(I) Photosensitizers $[Re(Cl)(CO)_3(N,N)]$ and $[Re(imidazole)(CO)_3(N,N)]^+$: Diimine Effects

Amal El Nahhas,[a] Cristina Consani,[a] Ana María Blanco-Rodríguez,[b] Kyle M. Lancaster,[c] Olivier Braem,[a] Andrea Cannizzo,[a] Michael Towrie,[d] Ian P. Clark,[d] Stanislav Záliš,*[,e] Majed Chergui,*[,a] Antonín Vlček, Jr.,*[,b,e]

[a] Laboratoire de Spectroscopie Ultrarapide, ISIC, FSB-BSP, Ecole Polytechnique Fédérale de Lausanne, CH-1015 Lausanne-Dorigny, Switzerland
[b] Queen Mary University of London, School of Biological and Chemical Sciences, Mile End Road, London E1 4NS, United Kingdom
[c] Beckman Institute, California Institute of Technology, Pasadena, CA 91125, USA
[d] Central Laser Facility, STFC Rutherford Appleton Laboratory, Chilton, Didcot, Oxfordshire OX11 0QX, United Kingdom
[e] J. Heyrovský Institute of Physical Chemistry, Academy of Sciences of the Czech Republic, Dolejškova 3, CZ-182 23 Prague, Czech Republic

e-mail: zalis@jh-inst.cas.cz, majed.chergui@epfl.ch, a.vlcek@qmul.ac.uk

Table S1. TD-DFT G03/PBE0/PCM-DMF calculated singlet electronic transitions of $[Re(imH)(CO)_3(N,N)]^+$ (top) and $[Re(Cl)(CO)_3(N,N)]$ (bottom) with oscillator strength larger than 0.001. Transition energies in eV, corresponding wavelengths (nm) in parenthesis. Molar absorptivities in $M^{-1}cm^{-1}$. Transitions originate in the a^1A' ground state. Relevant frontier orbitals are depicted in Figure S2.

State	Main components (%)	Calculated transitions	Osc. Str.	Expt. Transitions	Molar abs.
$[Re(imH)(CO)_3(phen)]^+$					
a^1A''	98 (HOMO→LUMO)	3.07 (404)	0.003		
b^1A'	72 (HOMO-1→LUMO) 20 (HOMO→LUMO+1) 7 (HOMO-2→LUMO)	3.37 (368)	0.054	3.40[a], 3.76 (~365, 330)	~4000
c^1A'	75 (HOMO-2→LUMO) 24 (HOMO-1→LUMO)	3.53 (351)	0.109		
g^1A''	Mixed π – π*	4.69 (264)	0.174	4.48 (277)	$\sim 2\times10^4$
f^1A'	Mixed π – π*	4.74 (262)	0.137		
h^1A''	Mixed π – π*	4.84 (256)	0.429		
$[Re(imH)(CO)_3(dmp)]^+$					
a^1A''	98 (HOMO→LUMO)	3.22 (384)	0.003		
c^1A'	52 (HOMO-1→LUMO) 24 (HOMO→LUMO+1) 23 (HOMO-2→LUMO)	3.56 (348)	0.118	3.40-3.87[a] (365-320)	
d^1A'	76 (HOMO-2→LUMO) 17 (HOMO-1→LUMO)	3.63 (341)	0.075		
b^1A''	90 (HOMO-1→LUMO+1)	3.74 (332)	0.066		
g^1A''	Mixed π – π*	4.69 (264)	0.256	4.49 (276)	
f^1A'	Mixed π – π*	4.71 (263)	0.194		
h^1A''	Mixed π – π*	4.84 (256)	0.392		
$[Re(imH)(CO)_3(bpy)]^+$					
a^1A''	97 (HOMO→LUMO)	3.03 (409)	0.004		
b^1A'	72 (HOMO-1→LUMO); 27 (HOMO-2→LUMO)	3.36 (369)	0.042	3.53[a] (351)	
c^1A'	73 (HOMO-2→LUMO); 26 (HOMO-1→LUMO)	3.46 (358)	0.067		
d^1A'	Mixed π – π*	4.32 (285)	0.029	3.86, 3.99 (321, 311)	
d^1A''	Mixed π – π*	4.34 (286)	0.259		

State	Main components (%)	Calculated transitions	Osc. Str.	Expt. transitions	Molar abs.
[Re(Cl)(CO)$_3$(phen)]					
a^1A“	98 (HOMO→LUMO)	2.97 (418)	0.002		
b^1A‘	90 (HOMO-1→LUMO) 10 (HOMO→LUMO+1)	3.13 (396)	0.077	3.39 (366)[a]	4000[b]
c^1A’	90 (HOMO→LUMO+1) 10 (HOMO-1→LUMO)	3.24 (371)	0.032		
b^1A”	95 (HOMO-1→LUMO+1)	3.44 (361)	0.023		
g^1A”	Mixed π – π*	4.71 (263)	0.073	4.25 (292sh)	
f^1A’	Mixed π – π*	4.78 (260)	0.085		
h^1A”	Mixed π – π*	4.85 (256)	0.469	4.61 (269)	30620[b]
[Re(Cl)(CO)$_3$(dmp)]					
a^1A“	98 (HOMO→LUMO)	3.11 (399)	0.002		
b^1A‘	71 (HOMO-1→LUMO) 27 (HOMO→LUMO+1)	3.24 (383)	0.059	3.48 (356)[a]	
c^1A’	71 (HOMO→LUMO+1) 27 (HOMO-1→LUMO)	3.34 (372)	0.071		
c^1A’	90 (HOMO-1→LUMO+1)	3.41 (364)	0.037		
g^1A”	Mixed π – π*	4.58 (271)	0.087	4.29, 4.59 (289sh, 270)	
f^1A’	Mixed π – π*	4.69 (264)	0.144		
h^1A”	Mixed π – π*	4.89 (254)	0.345	4.86 (255)	
[Re(Cl)(CO)$_3$(bpy)]					
a^1A“	98 (HOMO→LUMO)	2.94 (422)	0.003		
b^1A‘	97 (HOMO-1→LUMO)	3.12 (397)	0.078	3.35 (370)[a]	2450[c]
c^1A‘	90 (HOMO-1→LUMO+1)	4.20 (295)	0.043	3.90, 4.23 (318, 293)	
d^1A’	75 (HOMO-2→LUMO+1)	4.24 (292)	0.019		
e^1A’	75 (HOMO-2→LUMO+2)	4.40 (282)	0.029		
d^1A”	Mixed π – π*	4.44 (279)	0.358	4.88 (254)	

[a] Broad band tailing to ~430 nm. [b] From Worl, L. A.; Duesing, R.; Chen, P.; Della Ciana, L.; Meyer, T. J. *J. Chem. Soc. Dalton Trans.* **1991**, 849-858. [c] From Worl, L. A.; Duesing, R.; Chen, P.; Della Ciana, L.; Meyer, T. J. *J. Chem. Soc. Dalton Trans.* **1991**, 849-858.

Table S2. TD-DFT G03/PBE0/PCM-DMF calculated triplet electronic transitions of $[Re(imH)(CO)_3(N,N)]^+$ (top) and $[Re(Cl)(CO)_3(N,N)]$ (bottom). Transition energies in eV, corresponding wavelengths (nm) in parenthesis. Transitions originate in the a^1A' ground state. Relevant frontier orbitals are depicted in Figure S2.

State	Main components (%)	Calculated transitions
$[Re(imH)(CO)_3(phen)]^+$		
a^3A''	36 (HOMO→LUMO); 30(HOMO-4→ LUMO+1) 20 (HOMO-1→LUMO+1)	2.65 (467)
a^3A'	76 (HOMO-1→LUMO)	2.94 (422)
b^3A''	50 (HOMO→LUMO); 30(HOMO-4→ LUMO+1)	3.06 (406)
b^3A'	62 (HOMO-3→LUMO); 19(HOMO→ LUMO+1)	3.37 (367)
$[Re(imH)(CO)_3(dmp)]^+$		
a^3A''	34 (HOMO-1→LUMO+1) 34(HOMO-4→ LUMO+1) 29 (HOMO→ LUMO)	2.66 (467)
a^3A'	71 (HOMO-1→LUMO)	2.98 (416)
b^3A''	74 (HOMO→ LUMO)	3.14 (394)
b^3A'	81 (HOMO→ LUMO+1)	3.42 (362)
$[Re(imH)(CO)_3(bpy)]^+$		
a^3A''	74 (HOMO→LUMO); 21 (HOMO-4→ LUMO)	2.77 (448)
a^3A'	80 (HOMO-1→LUMO)	3.09 (401)
b^3A''	55 (HOMO-4→ LUMO); 25 (HOMO→LUMO)	3.17 (391)
b^3A'	91 (HOMO-2→ LUMO)	3.36 (369)

State	Main components (%)	Calculated transitions
$[Re(Cl)(CO)_3(phen)]$		
a^3A''	37 (HOMO→LUMO); 35(HOMO-4→ LUMO+1)	2.63 (470)
a^3A'	85 (HOMO-1→LUMO)	2.85 (435)
b^3A''	60 (HOMO→LUMO); 21(HOMO-4→ LUMO+1)	2.96 (418)
b^3A'	85 (HOMO-3→LUMO)	3.25 (381)
$[Re(Cl)(CO)_3(dmp)]$		
a^3A''	30 (HOMO-1→LUMO+1) 36(HOMO-4→ LUMO+1) 20 (HOMO→ LUMO)	2.63 (471)
a^3A'	73 (HOMO-1→LUMO)	2.91 (426)
b^3A''	78 (HOMO→ LUMO)	3.04 (407)
b^3A'	87 (HOMO→LUMO+1)	3.25 (381)
$[Re(Cl)(CO)_3(bpy)]$		
a^3A''	83 (HOMO→LUMO)	2.75 (451)
b^3A''	93 (HOMO-1→LUMO)	2.90 (427)
b^3A'	67 (HOMO-3→ LUMO+1); 22 (HOMO→LUMO)	3.13 (397)
b^3A'	92 (HOMO-2→LUMO)	3.37 (368)

Table S3. TD-DFT PBE0/PCM-DMF calculated triplet-triplet excitation energies (eV) for $[Re(imH)(CO)_3(N,N)]^+$ (top) and $[Re(Cl)(CO)_3(N,N)]$ (bottom) with oscillator strengths larger than 0.01. Transitions originate in the UKS-optimized lowest triplet a^3A.

$[Re(imH)(CO)_3(N,N)]^+$

N,N	Final State	Main contributing excitations	Assignment	Transition energy eV (nm)	Osc. Str.	Expt. eV (nm)
phen	b^3A	(90β → 93β)(89β → 93β)		0.72 (1720)	0.014	
	c^3A	(92β → 93β) (91β → 93β)		1.29 (959)	0.033	
	d^3A	(88α → 93α)		1.87 (664)	0.019	
	e^3A	(94α → 97α)	LMCT(phen$^{\bullet-}$, imH)	1.95 (635)	0.036	2.18-2.70 (570-460)
	f^3A	(94α → 99α)	LMCT(phen$^{\bullet-}$)	2.47 (502)	0.017	
	g^3A	(94α → 101α)	LMCT(phen$^{\bullet-}$, imH)	2.89 (429)	0.019	
	h^3A	(94α → 102α) (94α → 102α)	LMCT(phen$^{\bullet-}$)	2.93 (423)	0.063	
	i^3A	mixed	LMCT(phen$^{\bullet-}$, imH)	3.01 (411)	0.024	
	j^3A	(92β → 94β)	LMCT(phen$^{\bullet-}$)	3.12 (398)	0.031	~3.31 (~375)
	k^3A	(85α → 95α)	LMCT(phen$^{\bullet-}$, imH)	3.54 (351)	0.034	
	l^3A	(83α → 93α)	LMCT(phen$^{\bullet-}$, imH)	3.84 (323)	0.048	
	m^3A	Mixed	MLCT + ππ*(phen$^{\bullet-}$)	4.43 (279)	0.199	4.08 (304)
	n^3A	Mixed	MLCT + ππ*(phen$^{\bullet-}$)	4.48 (275)	0.275	
dmp	b^3A	(97β → 101β)(98β → 101β)		0.84 (1477)	0.010	
	c^3A	(97β → 101β)(99β → 101β)		1.24 (1001)	0.089	
	d^3A	(102α → 104α)		1.85 (668)	0.014	
	e^3A	(102α → 105α)	LMCT(dmp$^{\bullet-}$, imH)	1.97 (630)	0.045	2.18-2.76 (570-450)
	f^3A	(102α → 107α)	LMCT(dmp$^{\bullet-}$)	2.54 (502)	0.025	
	g^3A	(94β → 101β)	LMCT(dmp$^{\bullet-}$)	2.84 (436)	0.021	
	h^3A	(94α → 101α)	LMCT(dmp$^{\bullet-}$)	2.89 (429)	0.019	
	i^3A	(102α → 109α) (102α → 110α)	LMCT(dmp$^{\bullet-}$, imH)	2.91 (426)	0.103	
	j^3A	mixed	LMCT(dmp$^{\bullet-}$, imH)	3.04 (408)	0.023	
	k^3A	(93β → 101β)	LMCT(dmp$^{\bullet-}$)	3.27 (378)	0.015	
	l^3A	(102α → 113α)	LMCT(dmp$^{\bullet-}$, imH)	3.49 (355)	0.022	
	m^3A	(100β → 102β)(100β → 103β)	LMCT(dmp$^{\bullet-}$, imH)	3.61 (343)	0.033	
	n^3A	Mixed	MLCT + ππ*(dmp$^{\bullet-}$)	4.24 (292)	0.133	4.08 (304)
	o^3A	Mixed	MLCT + ππ*(dmp$^{\bullet-}$)	4.26 (291)	0.071	
	p^3A	Mixed	MLCT + ππ*(dmp$^{\bullet-}$)	4.39 (282)	0.292	
bpy	b^3A	(85α → 86α)		1.03 (1200)	0.010	
	c^3A	(88α → 90α)		1.60 (774)	0.018	
	d^3A	(88α → 91α)		1.66 (745)	0.035	
	e^3A	(88α → 94α)	LMCT(bpy$^{\bullet-}$)	2.01 (617)	0.044	
	g^3A	(88α → 93α)(80β → 87β)	LMCT(bpy$^{\bullet-}$)	2.79 (444)	0.019	2.75, 2.92 (451, 425)
	h^3A	(88α → 93α)(80β → 87β)	LMCT(bpy$^{\bullet-}$)	2.82 (439)	0.024	
	i^3A	(88α → 99α)(86β → 88β)	LMCT(bpy$^{\bullet-}$, imH)	3.12 (397)	0.030	
	k^3A	Mixed	ππ*(bpy$^{\bullet-}$) + MLCT	3.59 (345)	0.146	3.38 (367)
	l^3A	Mixed	ππ*(bpy$^{\bullet-}$) + MLCT	3.65 (340)	0.304	

$[Re(Cl)(CO)_3(N,N)]$

N,N	Final State	Main contributing excitations	Assignment	Transition energy eV (nm)	Osc. Str.	Expt. eV (nm)
phen	b^3A	$(85\alpha \rightarrow 86\alpha)$		0.75 (1645)	0.012	
	c^3A	$(82\beta \rightarrow 84\beta)$ $(83\beta \rightarrow 84\beta)$		1.37 (906)	0.040	
	d^3A	$(85\alpha \rightarrow 87\alpha)$		1.87 (664)	0.025	
	e^3A	$(85\alpha \rightarrow 88\alpha)$	LMCT(phen$^{\bullet-}$, Cl)	1.98 (626)	0.029	2.64, 2.19 (470, 565sh)
	f^3A	$(79\beta \rightarrow 84\beta)$	LMCT(phen$^{\bullet-}$)	2.46 (504)	0.015	
	g^3A	$(85\alpha \rightarrow 91\alpha)$	LMCT(phen$^{\bullet-}$, Cl)	2.68 (463)	0.028	
	h^3A	$(85\alpha \rightarrow 92\alpha)$	LMCT(phen$^{\bullet-}$)	2.77 (447)	0.035	
	i^3A	mixed	LMCT(phen$^{\bullet-}$, Cl)	3.12 (398)	0.027	
	j^3A	$(85\alpha \rightarrow 95\alpha)$	LMCT(phen$^{\bullet-}$)	3.31 (375)	0.060	
	k^3A	Mixed	LMCT(phen$^{\bullet-}$, Cl)	3.65 (339)	0.016	4.13, 4.04, 3.97 (300sh, 307, 312sh)
	l^3A	Mixed	LMCT(phen$^{\bullet-}$, Cl)	3.68 (337)	0.015	
	m^3A	Mixed	MLCT + $\pi\pi^*$(phen$^{\bullet-}$)	4.25 (292)	0.036	
	n^3A	Mixed	MLCT + $\pi\pi^*$(phen$^{\bullet-}$)	4.35 (285)	0.162	
	o^3A	Mixed	$\pi\pi^*$(phen$^{\bullet-}$)	4.54 (273)	0.110	
dmp	b^3A	$(93\alpha \rightarrow 94\alpha)$		0.65 (1906)	0.007	
	c^3A	$(90\beta \rightarrow 92\beta)(91\beta \rightarrow 92\beta)$		1.32 (940)	0.056	
	d^3A	$(93\alpha \rightarrow 95\alpha)$		1.79 (691)	0.025	
	e^3A	$(93\alpha \rightarrow 96\alpha)$	LMCT(dmp$^{\bullet-}$, Cl)	1.89 (657)	0.032	
	f^3A	$(93\alpha \rightarrow 98\alpha)$	LMCT(dmp$^{\bullet-}$)	2.52 (492)	0.027	2.65, 2.19 (467, 565sh)
	g^3A	$(86\beta \rightarrow 92\beta)$	LMCT(dmp$^{\bullet-}$)	2.63 (472)	0.017	
	i^3A	$(93\alpha \rightarrow 101\alpha)$	LMCT(dmp$^{\bullet-}$, Cl)	2.79 (444)	0.068	
	j^3A	$(85\beta \rightarrow 92\beta)$	LMCT(dmp$^{\bullet-}$, Cl)	3.07 (404)	0.026	
	k^3A	$(84\beta \rightarrow 92\beta)$	LMCT(dmp$^{\bullet-}$)	3.24 (383)	0.034	
	l^3A	$(93\alpha \rightarrow 103\alpha)$	LMCT(dmp$^{\bullet-}$, Cl)	3.28 (378)	0.048	
	m^3A	$(100\beta \rightarrow 102\beta)(100\beta \rightarrow 103\beta)$	LMCT(dmp$^{\bullet-}$, Cl)	3.68 (337)	0.013	4.13, 4.04, 3.97 (300sh, 307, 312sh)
	n^3A	Mixed	MLCT + $\pi\pi^*$(dmp$^{\bullet-}$)	4.16 (298)	0.074	
	o^3A	Mixed	MLCT + $\pi\pi^*$(dmp$^{\bullet-}$)	4.24 (292)	0.058	
	p^3A	Mixed	$\pi\pi^*$(dmp$^{\bullet-}$)	4.29 (289)	0.051	
bpy	b^3A	$(77\beta \rightarrow 78\beta)$		1.14 (1091)	0.009	
	c^3A	$(79\alpha \rightarrow 80\alpha)$		1.53 (807)	0.026	
	d^3A	$(79\alpha \rightarrow 82\alpha)$		1.63 (763)	0.032	
	e^3A	$(74\beta \rightarrow 78\beta)$	LMCT(bpy$^{\bullet-}$)	2.35 (526)	0.030	2.58 (480)
	f^3A	$(79\alpha \rightarrow 84\alpha)$	LMCT(bpy$^{\bullet-}$)	2.64 (470)	0.014	
	g^3A	$(79\alpha \rightarrow 85\alpha)$	LMCT(bpy$^{\bullet-}$)	2.73 (455)	0.013	
	h^3A	$(79\alpha \rightarrow 89\alpha)$	LMCT(bpy$^{\bullet-}$, Cl)	3.03 (409)	0.041	
	i^3A	Mixed	LMCT + $\pi\pi^*$(bpy$^{\bullet-}$)	3.53 (351)	0.114	3.32 (373)
	j^3A	Mixed	LMCT + $\pi\pi^*$(bpy$^{\bullet-}$)	3.62 (342)	0.294	

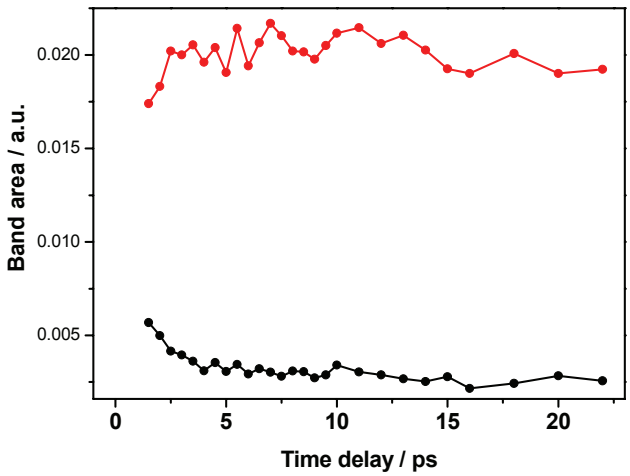

Figure S1. Time dependence of the band area of the minor (black) and major (red) excited-state A'(1) bands of [Re(Cl)(CO)$_3$(dmp)]. Data obtained by band-shape fitting of the TRIR spectra, see the text.

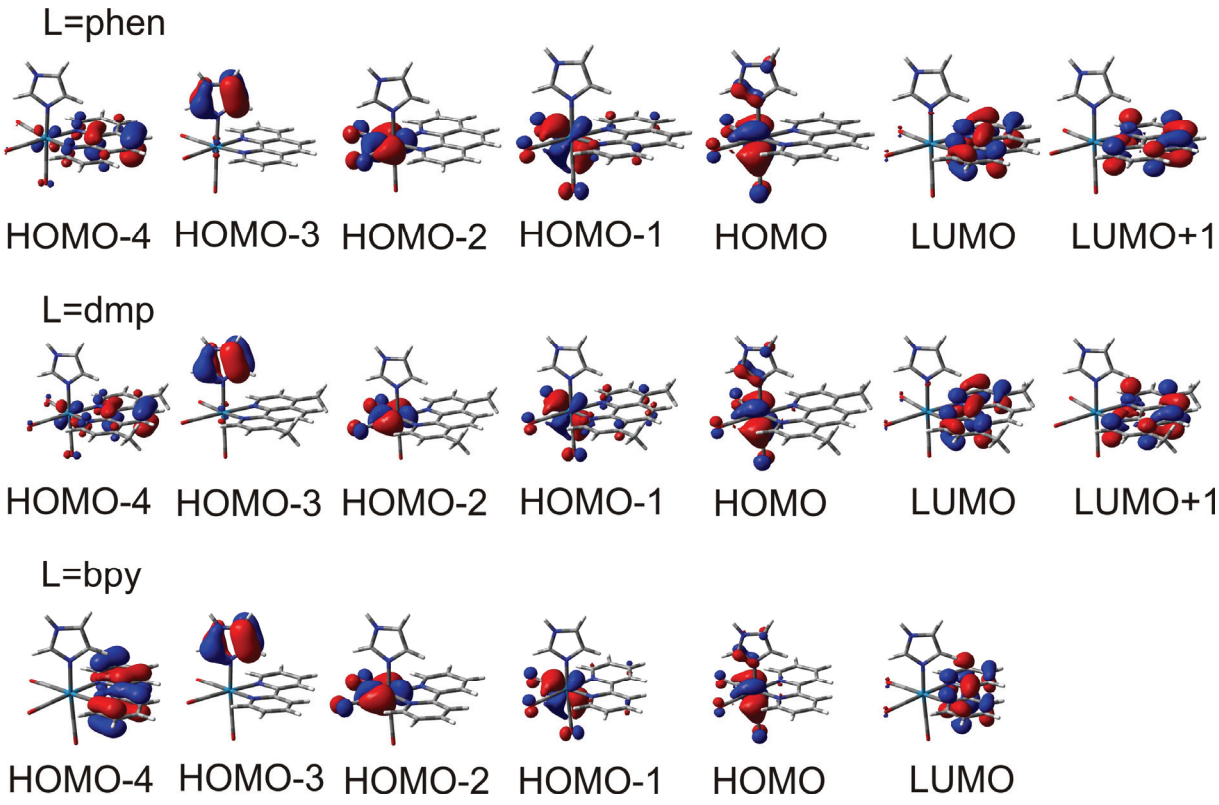

Figure S2A. Frontier molecular orbitals involved in TD DFT calculated lowest singlet and triplet transitions of [Re(im)(CO)$_3$(dmp)]$^+$ (bottom) presented in Tables S1 and S2. PBE0/PCM(for DMF) calculation. MO's of other investigated imH complexes are similar.

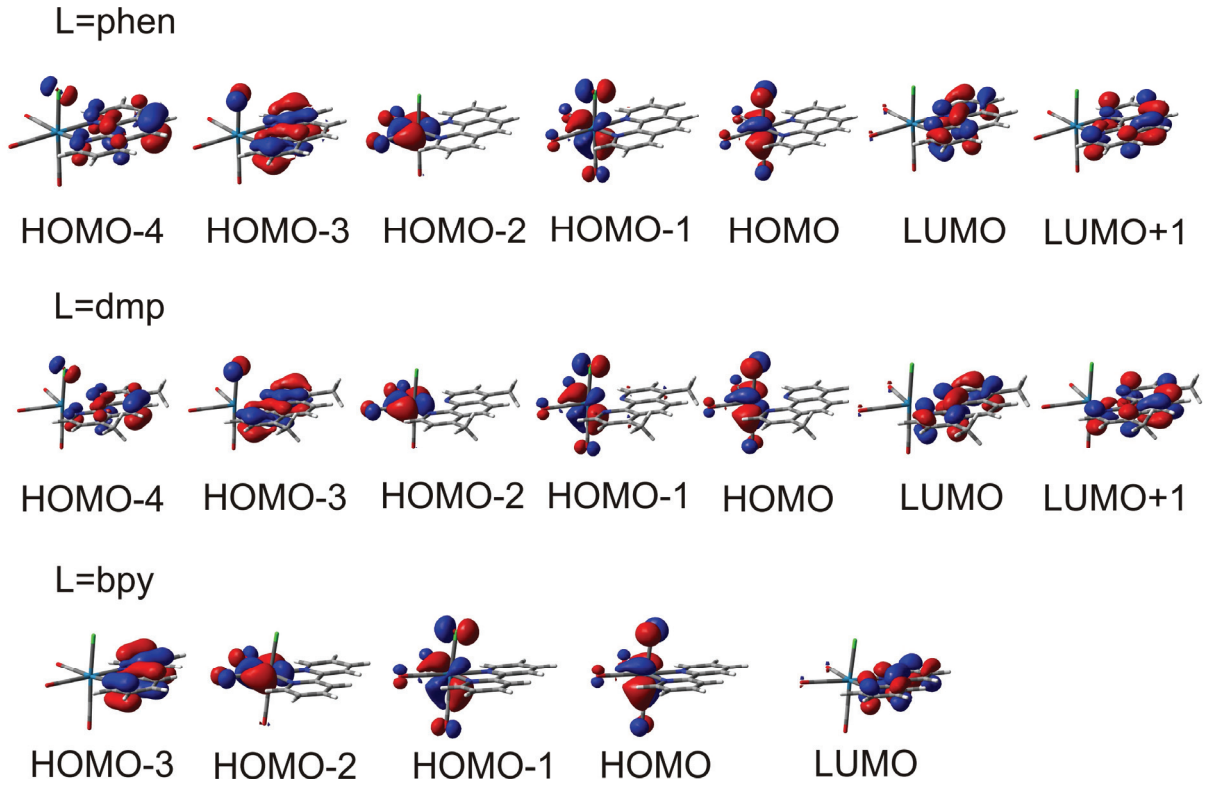

Figure S2B. Frontier molecular orbitals involved in TD DFT calculated lowest singlet and triplet transitions of [Re(Cl)(CO)$_3$(N,N)] presented in Tables S1 and S2. PBE0/PCM(for DMF) calculation. MO's of other investigated imH complexes are similar.

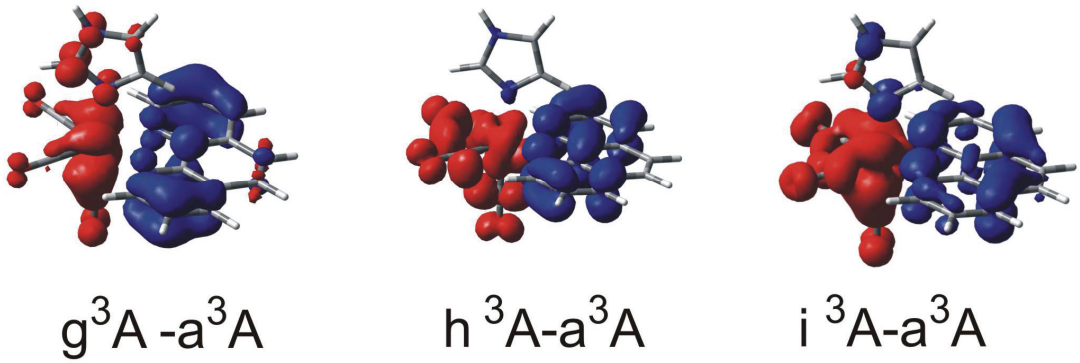

Figure S3. Electron-density differences upon three intense transitions from the lowest triplet state a^{3}A of [Re(imH)(CO)$_3$(phen)]$^+$, expected in the visible part of the TA spectrum. Regions of decreasing and increasing electron density are displayed in blue and red, respectively. The transitions are described in Table S3. TD DFT (PBE0/PCM-DMF) calculation.

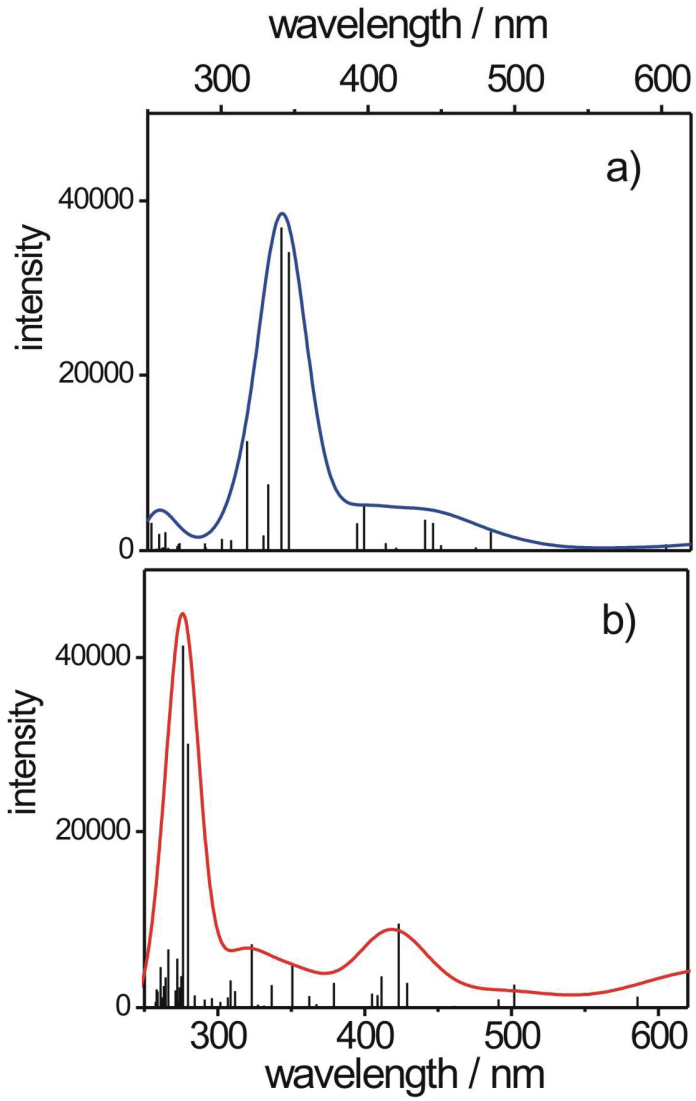

Figure S4. Comparison of simulated UV-vis excited-state absorption spectra of a) $[Re(imH)(CO)_3(bpy)]^+$, b) $[Re(imH)(CO)_3(phen)]^+$. Open-shell TD-DFT (PBE0/CPCM-DMF), included all transitions calulated in the range 200 - 800 nm, 0.3 fwhm.

Gaussian full reference:

(46) Frisch, M. J.; Trucks, G. W.; Schlegel, H. B.; Scuseria, G. E.; Robb, M. A.; Cheeseman, J. R.; Scalmani, G.; Barone, V.; Mennucci, B.; Petersson, G. A.; Nakatsuji, H.; Caricato, M.; Li, X.; Hratchian, H. P.; Izmaylov, A. F.; Bloino, J.; Zheng, G.; Sonnenberg, J. L.; Hada, M.; Ehara, M.; Toyota, K.; Fukuda, R.; Hasegawa, J.; Ishida, M.; Nakajima, T.; Honda, Y.; Kitao, O.; Nakai, H.; Vreven, T.; Montgomery, J. A., Jr.; Peralta, J. E.; Ogliaro, F.; Bearpark, M.; Heyd, J. J.; Brothers, E.; Kudin, K. N.; Staroverov, V. N.; Kobayashi, R.; Normand, J.; Raghavachari, K.; Rendell, A.; Burant, J. C.; Iyengar, S. S.; Tomasi, J.; Cossi, M.; Rega, N.; Millam, J. M.; Klene, M.; Knox, J. E.; Cross, J. B.; Bakken, V.; Adamo, C.; Jaramillo, J.; Gomperts, R.; Stratmann, R. E.; Yazyev, O.; Austin, A. J.; Cammi, R.; Pomelli, C.; Ochterski, J. W.; Martin, R. L.; Morokuma, K.; Zakrzewski, V. G.; Voth, G. A.; Salvador, P.; Dannenberg, J. J.; Dapprich, S.; Daniels, A. D.; Farkas, O.; Foresman, J. B.; Ortiz, J. V.; Cioslowski, J.; Fox, D. J. *Gaussian 09, Revision A.02*, Gaussian 09, Revision A.02, Gaussian, Inc.: Wallingford CT, 2009.